Journal of Environmental Management 373 (2025) 123357

Contents lists available at ScienceDirect

Journal of Environmental Management

journal homepage: www.elsevier.com/locate/jenvman

Research article

Carbon dioxide and methane gas exchange following sphagnum moss harvesting in boreal peatland

Satu K. Karjalainen [a,*], Jani Anttila [a], Liisa Maanavilja [b], Alireza Hamedianfar [b], Anna M. Laine [c,b]

[a] Natural Resources Institute Finland (Luke), Latokartanonkaari 9, 00790 Helsinki, Finland
[b] Geological Survey of Finland (GTK), Vuorimiehentie 5, 02151 Espoo, Finland
[c] University of Eastern Finland (UEF), Tulliportinkatu 1, 80130 Joensuu, Finland

ARTICLE INFO

Keywords:
Peatland
Sphagnum
CO_2 flux
CH_4 emissions
Vegetation recovery
Hydrology
UAV imagery

ABSTRACT

Understanding the impacts of *Sphagnum* moss harvesting on peatland carbon (C) balance is crucial due to its potential rise as an anthropogenic land use. We studied eight nutrient-poor peatlands in Finland, harvested between 2015 and 2021, focusing on net ecosystem exchange of CO_2 (NEE) and methane (CH_4) emissions. The greenhouse gas fluxes were measured to evaluate the sustainability of harvesting practices. Results showed significant variability in *Sphagnum* regeneration, with wet strip-harvested sites achieving 2–28% re-establishment in 2–8 years, while drier clear-harvested sites saw minimal spontaneous regeneration in 1–6 years. In addition to vegetation succession, GHG emissions were moisture dependent. In wet sites CH_4 emissions increased along with time since harvesting and *Eriophorum vaginatum* (L.) cover, while dry sites exhibited overall lower CH_4 fluxes. Younger (1–2 years post-harvest), dry sites were significant CO_2 sources due to low photosynthetic activity. Older dry site with sparse ericoid shrub vegetation acted as CO_2 sink. Wet sites initially had lower CO_2 sink capacity, but this increased as *E. vaginatum* spread, and reached a plateau when *Sphagnum* mosses emerged, highlighting the importance of suitable water table levels for efficient CO_2 sequestration.

1. Introduction

Climate change is challenging open field cultivation, necessitating increased food production to meet the demands of a growing global population (Anderson et al., 2020). In greenhouse cultivation, where vegetable production is shielded from extreme weather events, horticultural peat is the primary growth substrate (Kitir et al., 2018). However, peat extraction leads to high CO_2 emissions (Sarauer and Coleman, 2018; Upenieks and Rudusāne, 2022) and peat is not considered renewable due to the slow regeneration process. With peatlands storing around 500 ± 100 billion tonnes of carbon globally (Yu, 2012), human activities can quickly deplete these long-term carbon stores (Leifeld et al., 2019). Therefore, it is crucial to explore alternative growing media substrates, such as the *Sphagnum* moss, which might be a more carbon-conscious option.

Sphagnum moss has been studied as an alternative to peat-based growing media (Gruda, 2019; Tommila et al., 2022). In Finland, instead of *Sphagnum* cultivation, existing *Sphagnum* mosses have been harvested from hydrologically degraded peatlands where the peat layer is considered too shallow for peat production or forestry-drainage has failed to initiate productive tree growth. As such areas cover nearly a million hectares in Finland (Laiho et al., 2016), potential for *Sphagnum* harvesting exists. However, its impacts on vegetation and GHG exchange are still little studied. Based on existing studies, harvesting depth impacts the resulting GHG exchange: shallow harvesting (less than 25 cm) allowed peatlands to become carbon sinks within three years with minor CH_4 emissions, while deeper harvesting (25–50 cm) reduced carbon sequestration and increased CH_4 emissions (Silvan et al., 2012). In addition, interannual variation may turn a harvested site from a sink to a source of CO_2 (Silvan et al., 2017). These previous studies, focusing on pioneering harvesting experiments, are carried out in sites with shallower harvesting and smaller or discontinuous harvesting areas compared to current industrial practices, which involve deep (30–50 cm) harvesting and larger areas, leaving little *Sphagnum* for regeneration.

The current form of *Sphagnum* harvesting leaves peatlands barren,

* Corresponding author.
E-mail address: satu.karjalainen@luke.fi (S.K. Karjalainen).

https://doi.org/10.1016/j.jenvman.2024.123357
Received 15 August 2024; Received in revised form 21 October 2024; Accepted 12 November 2024
Available online 26 November 2024

initiating a vegetation succession process where species gradually return, changing the plant composition over decades. The successional development of vegetation has, however, not been studied. The site conditions after Sphagnum harvesting resemble those of cutover peatlands where horticultural peat extraction involved removing the upper, undecomposed peat layer, has commenced. Vegetation re-establishment on cutover peatlands depends on water table level, initial vegetation coverage, temperature, and nutrient status (Strack et al., 2014). Strack et al. (2014) found no spontaneous recolonization on abandoned peatlands, however, when such sites are actively and successfully restored using the moss layer transfer technique vegetation recovery may be swift (González-Sargas, E. & Rochefort, L., 2019). Greenhouse gas exchange is strongly linked to vegetation structure (Kuiper et al., 2014; Peichl et al., 2018; Laine et al., 2022). For example, gas exchange alters significantly along with the vegetation type during natural peatland succession (Leppälä et al., 2008, 2011) and restored cutaway peatlands may shift from bare peat surfaces acting as net CO_2 sources to fully vegetated carbon sinks within ten years, with *Sphagnum*-covered surfaces having low or negligible CH_4 emissions and *E. vaginatum*-covered surfaces being CH_4 sources, with both acting as CO_2 sinks (Nugent et al., 2018, 2021). Therefore, after *Sphagnum* harvesting GHG exchange could be expected to change in time following vegetation succession.

The coexistence of graminoids and *Sphagnum* mosses can stabilize CO_2 exchange, making restored peatlands larger CO_2 sinks than when either is present alone (Kivimäki et al., 2008). *Sphagnum* mosses with methane-oxidizing bacteria have been shown to significantly reduce CH_4 emissions (Kox et al., 2021), while graminoid (*E. vaginatum*) covered surfaces are known to significantly increase CH_4 emissions post-restoration, as graminoid vegetation can enhance CH_4 production by providing labile substrates in anoxic zones and transporting CH_4 through aerenchymatous tissue (Greenup et al., 2000; Waddington and Day, 2007; Strack et al., 2016). However, in extreme cases with very high coverage, aerenchymatous vegetation can also aerate saturated soil, reducing CH_4 emissions (Fritz et al., 2011).

This study investigates the development of net CO_2 exchange and CH_4 emissions over seven years following *Sphagnum* harvesting in nutrient-poor peatlands. We hypothesize that gas fluxes are connected to changes in vegetation composition. Specifically, CH_4 emissions are lowest in the first post-harvest years due to the absence of vegetation and fluctuating water table levels, increasing as aerenchymatous graminoid vegetation develops. Initially, harvested peatlands act as CO_2 sources due to the lack of photosynthesis, but as pioneer vascular vegetation establishes, they become CO_2 sinks. We also hypothesize that methane emissions and CO_2 sinks are influenced by water table levels, with higher water tables leading to higher methane emissions and stronger CO_2 sinks.

2. Materials and methods

2.1. Study sites and Experimental design

The study was conducted at eight originally *Sphagnum*-dominated, oligo- or ombrotrophic peatland sites located in the South Ostrobothnia and Pirkanmaa regions of Finland (Table 1). The hydrology of these sites had been altered by nearby peat production activities, road construction, or forestry drainage. Three of the sites were specifically drained for forestry, but tree growth had been unsuccessful (Table 1). *Sphagnum* harvesting had been performed on sites, which varied by harvesting year and harvesting method (Table 1, Fig. S1.1 and Fig. S1.2).

During the study years of 2022 and 2023, the average annual temperatures were 5.2 °C and 4.7 °C, respectively, while the seasonal (April–October) average temperatures were 12.2 °C and 12.3 °C, respectively (Weather Station, Seinäjoki Peijaa). The temperature in 2022 deviated more from the region's 30-year (1991–2020) average of 4.6 °C. Both 2022; 2023 seasonal temperature averages were nearly 2 °C higher than the 30-year average of 10.4 °C. Annual precipitation in 2022 was 703 mm, with the preceding winter months (December–February) receiving 86.7 mm of precipitation. In 2023, annual precipitation decreased to 686 mm, although the preceding winter months experienced higher precipitation of 109 mm. Both 2022; 2023 annual precipitation totals were significantly higher than the 30-year average of 561 mm. The 30-year average precipitation for winter months is 64.4 mm, indicating an increase in rainfall events in 2022 and 2023.

2.2. GHG flux measurements and Ancillary measurements

CO_2 and CH_4 exchange measurements were carried out using the chamber method from June to October of 2022 and from April to October of 2023, at intervals of 2–3 weeks. Each site was designed with two treatment types: harvested and control, each containing five sampling points for gas exchange measurements. This setup results in ten total measurement points per site, providing five pseudo-replicate measurements for each treatment type within a site. Therefore, the unit of replication for our analyses is defined as the site (harvested vs. control).

Wooden broadwalks were installed next to sample plots to prevent disturbances in the gas fluxes caused by the movements of the measurers. A slit was made around each sample plot with scissors to ensure the chamber fit tightly against the ground. The flux development was followed while measuring and the chamber was aerated between the measurements to ensure that the ambient ~400 parts per million (ppm; Ma et al., 2020) air CO_2 level was reached before starting the next measurement.

Carbon dioxide (CO_2) and methane (CH_4) exchange was measured using a transparent plastic cylinder shaped chamber (40 cm height, 40 cm diameter) connected to a portable trace gas analyzer (LI-7810, LI-COR Biosciences, USA). The two chambers used were equipped with a fan and either a thermostatic cooling system or a Peltier cooling component, both of which maintained the chamber air temperature within ±2 °C of ambient conditions (Alm et al., 2007).

The measurement routine at each plot consisted of four measurements lasting between 60 and 180 s. First, gas exchange was measured under stable full ambient light. Next, measurements were taken under one or two shades that reduced incoming light to approximately 2/3 and 1/3 of ambient levels, respectively. Finally, the chamber was covered with an opaque hood for the dark measurement. The chamber was

Table 1
Study site location, used harvesting method, post-harvest years (calculated from 2022), and the harvested and control surface areas. An asterisk (*) indicates forestry-drainage sites/close proximity of forestry-drainage site. In clear-harvested sites, most of the peatland surface has been evenly harvested, leaving large bare peat areas, while at strip-harvested sites, strips of unharvested surfaces remain between harvested areas (see Fig. S1.1 and Fig. S1.2 for more details).

Site	Location	Harvesting method	Years post-harvest (harvesting year)	Harvested area (ha)	Unharvested area (ha)
Ylimysneva*	62.148 °N, 22.869 °E	Clear-harvested	1 (2021)	2.0	0.5
Kivisalmenneva south	62.442 °N, 23.266 °E	Clear-harvested	2 (2020)	14.4	2.1
Tuuraneva*	62.350 °N, 23.342 °E	Clear-harvested	2 (2020)	3.5	0.2
Liminganneva	62.433 °N, 23.284 °E	Strip-harvested	4 (2018)	5.4	3.8
Kivisalmenneva north	62.445 °N, 23.263 °E	Strip-harvested	5 (2017)	0.9	1.1
Peurainneva	62.359 °N, 23.185 °E	Clear-harvested	5 (2017)	9.1	4.8
Hoikkasuolenneva	62.201 °N, 23.276 °E	Strip-harvested	7 (2015)	3.5	5.4
Nimetonneva*	62.131 °N, 23.516 °E	Strip-harvested	7 (2015)	1.2	2.5

ventilated between each measurement.

Simultaneously with gas flux measurements, photosynthetic photon flux density (PPFD) and air temperature inside the chamber were recorded. Three light measuring sensors were used and calibrated under laboratory conditions to harmonize light levels: LI-1500 (LI-COR Biosciences, USA), LI-250A (LI-COR Biosciences, USA), and a radiation sensor attached to an EGM-4 infrared gas analyzer (PP Systems, UK). Additionally, soil temperature at 5 cm and 20 cm depths and water table level (WTL) were measured adjacent to each sample plot. For water table measurement, a perforated tube was permanently installed next to each plot.

To monitor the seasonal development of photosynthesizing greenness in the sample plots, photographs were taken with a Samsung Galaxy A32 phone camera at each measurement time. The camera was positioned 1 m above the sample point, and a 40 cm diameter metallic ring delineated the region of interest (ROI). The photographs were scaled and cropped using ImageJ software, and then stored in JPEG format with red, green, and blue (RGB) digital numbers (DN) for each pixel.

To reduce variability in daylight affecting RGB brightness levels (Woebbecke et al., 1995), RGB numeric values were transformed into chromatic coordinates (Sonnentag et al., 2012). The green chromatic coordinate (GCC) is calculated using the formula:

$$\mathrm{GCC} = \frac{G}{\mathrm{R} + \mathrm{G} + \mathrm{B}} \tag{1}$$

where R, G, and B are the per-pixel digital numbers stored in the image, recorded as intensity values. GCC was computed for each pixel of the image and averaged over the region of interest. This method has been effective in detecting seasonal phenological changes in plant leaves, such as color and leaf surface area, and is considered a good indicator of CO_2 sequestration by peatland vegetation (Peichl et al., 2018; Sonnentag et al., 2012). The analysis was conducted using the R statistical computing environment (R Core Team, 2020) with the Phenopix package.

2.3. Vegetation survey and sample plot grouping

In June/July 2022, vegetation within the sample plots was surveyed to determine the percentage cover of vascular plants, mosses, and lichens at the species level, as well as bare peat surface area. Vegetation was surveyed from the same sampling points from where the gas fluxes were measured, with the same 40 cm radius. The cover of each plant species was visually estimated to the precision of one percentage point, or to 0.1 percentage point for covers under 1%. The sample plots were then grouped based on vegetation composition using t-distributed stochastic neighbor embedding (t-SNE; van der Maaten and Hinton, 2008; van der Maaten, 2014).T-SNE is a dimensionality reduction technique that maps high-dimensional data points to a lower-dimensional space while preserving pairwise similarities between them. For t-SNE clustering, the vegetation percentage data from the sample plots underwent Hellinger transformation, and a distance matrix was computed using the Bray-Curtis method. To validate the t-SNE clustering results, a traditional distance-based ordination technique, Non-metric Multidimensional Scaling (NMDS), was performed using the Hellinger-transformed species percentage data from the sample plots. Visualization of both t-SNE and NMDS results was conducted using the R statistical computing environment (R Core Team, 2020) with the Rtsne and vegan packages. These analyses facilitated the grouping and visualization of sample plots based on their vegetation composition, providing insights into the similarities and dissimilarities among different plots within the study area.

2.4. GHG flux data processing and statistical analysis

The carbon dioxide (CO_2) and methane (CH_4) fluxes for each measurement were calculated based on the linear change (slope) in gas concentration over time, considering chamber volume and temperature. The flux values were calculated using the equation:

$$f = s \bullet \frac{M}{V_m} \bullet \frac{T_o}{T_o + T} \bullet \frac{V}{A} \bullet c$$

where s is the fitted slope, M is molar mass of the measured gas, T is the arithmetic mean of chamber temperatures at measurement start and measurement end, V is chamber volume, A is chamber area, $T_o = 273.15$ K, $c = 3600$ is conversion factor from s^{-1} to h^{-1}, and $V_m = RT_o/p$, where R is the molar gas constant, and a constant pressure $p = 101{,}325$ Pa is assumed.

Each measurement was visually inspected for quality control and trimmed if necessary. Nonlinear changes in concentration, indicative of abnormalities such aschamber leaks (for CH_4 and CO_2), or soil pressure change caused by the measurer were identified and excluded. A total of 4531 measurements were included in the analysis and $\leq$5 % of the measurements were excluded.

Statistical analysis and data visualization were performed using the R statistical computing environment (R Core Team, 2020), with the ggplot2 package (Wickham, 2016) used specifically for data visualization. Statistical tests were carried out on the individual measurements without considering the surface area normalization of vegetation types (section 2.5). One possible source of error in the related conclusions is that the individual measurement points did not represent the vegetation types on the sites in the correct proportions.

Cumulative seasonal CH_4 fluxes were calculated using trapezoidal integration, which involved linear interpolation between measurements followed by summation of consecutive daily values.

Hourly Net Ecosystem Exchange (NEE) values were derived by fitting a statistical model to the photosynthetic light-response curve. The NEE modeling approach aligns with methodologies described in Korrensalo et al. (2020a, 2020b) and Laine et al. (2019). Compared to these previous works, our NEE model utilised GCC as a covariate instead of leaf area index (LAI). Additionally, our model was simplified with respect to the number of included random factors (*i.e.* hierarchy levels). The NEE model can be expressed as:

$$NEE_{ij}(t) = \frac{Pmax_{ij} \bullet PPFD(t)}{\alpha + PPFD(t)} - R_{ij} \tag{2}$$

In the equation $NEE_{ij}(t)$ is the observed net CO_2 exchange for plot i in site j at time (hour) t. The $NEE_{ij}(t)$ is calculated from a photosynthetic production term, which follows the saturating Michaelis-Menten curve with respect to the photosynthetically active photon flux density PPFD(t), and an ecosystem respiration term R_{ij}. The parameters $Pmax_{ij}$ and R_{ij} of the photosynthesis term consist of sub-models:

$$Pmax_{ij}(t) = exp\left(\beta_0 + \beta_i + \beta_j + \beta_1 GCC_{ij}(t) + \beta_2 T_{ij}(t) + \beta_3 WT_{ij}(t)\right) \tag{3}$$

$$R_{ij}(t) = exp\left(\gamma_0 + \gamma_i + \gamma_j + \gamma_1 GCC_{ij}(t) + \gamma_2 T_{ij}(t) + \gamma_3 WT_{ij}(t)\right) \tag{4}$$

where $GCC_{ij}(t)$ is the green chromatic coordinate at plot i in site j at time t, $T_{ij}(t)$ is air temperature, and $WT_{ij}(t)$ is water table level. Instead of leaf area index used in most of the previous works, we used the green chromatic coordinate (GCC) as a covariate representing the amount of photosynthetic plant material in our model.

The model parameters were fitted under the Bayesian paradigm using the no-u-turn HMC sampler implemented in Stan (Stan Development Team, 2024) via the RStan interface. Informative priors were used based on previous works (Korrensalo et al., 2020a, 2020b; Laine et al., 2019) and the reasonable distributions for each parameter were evaluated, which mitigated parameter identifiability issues due to the relatively large number of parameters in the model. The parameters for the NEE model, our prior distributions and estimates from the posterior distribution are listed in supplementary information Table S1.1.

Positive NEE values indicate the ecosystem's uptake of CO_2 from the

atmosphere, while negative NEE values indicate the emissions of CO_2 from the ecosystem to the atmosphere. The positive CH_4 values represent emissions to the atmosphere.

The fitted statistical model for was used for calculating the hourly flux values for each measurement point. To facilitate this process the Green Chromatic Coordinate (GCC) and water table level (WTL) values were calculated for each measurement point and day within the measurement season using linear interpolation between measurements. To address missing data from the initial part of 2022, values were extrapolated based on observed changes in GCC and WTL during the corresponding period in 2023. Hourly PPFD and air temperature data were continuously measured at a weather station installed at the Liminganneva site. Data gaps were filled by Seinäjoki, Peijaa weather station.

2.5. Surface area normalization of the vegetation types

To facilitate comparisons of greenhouse gas fluxes across different sites and treatments, surface area normalization was performed to account for variations in the spatial extent of vegetation types (PCTs) represented by the different gas flux sample plots. The site-specific cover of vegetation types was obtained through aerial imaging.

A digital surface model (DSM) and multispectral imagery acquired via unmanned aerial systems (UAS) were used to map the vegetation of the sites using random forest supervised classification. A WingtraOne fixed-wing UAV, equipped with a Sony RX1RXII 42 MP camera (field of view 50°) and post-kinematic processing (PPK), was used to obtain 1) the DSM and 2) an RGB ortophoto for georectifying the multispectral imagery. A MicaSense Altum multispectral camera (field of view 50° vertically and 38° horizontally) was employed to acquire the multispectral images, including blue, green, red, red edge, near-infrared (NIR), and long-wave infrared (LWIR) bands, with a 5 cm spatial resolution. We applied georeferencing on the multispectral imagery to the a Sony RX1RXII RGB ortophoto to ensure spatial accuracy.

The UAV flights were conducted in stable light conditions, either with uniform cloud cover or full sunlight. The vegetation at the sites was mostly of low stature, thus the shadows resulting from full light did not have a large impact on the classification results. Ambient light calibration was performed using a calibration panel at the start of each flight. Since classification was done separately for each site, variations in light conditions between sites did not affect the classification results.

The following categories were used in the supervised image classification: 1) bare peat, 2) water, 3) Calluna (*Calluna vulgaris* (L.) Hull and other occasional dwarf shrubs), 4) Eriovagi (*E. vaginatum*), 5) *Carex*, 6) hummock *Sphagnum* (red), 7) lawn *Sphagnum* (yellowish), and 8) shrubs and trees. These categories were selected based on a field survey of the sites. Approximately 100 ground-truth points per site were collected in the field, and the number was further increased manually to around 100 points per vegetation category based on visual interpretation of very high spatial resolution orthophoto images of the study sites.

Classification of vegetation classes from the multispectral and DSM images was conducted in Python using the Scikit-learn implementation of the random forest classification algorithm (Pedregosa et al., 2012). The field data were used to train the classification model, and 5-fold cross-validation was applied to evaluate the model's performance.

The surface areas of the classified vegetation types from the UAV imagery were matched with the sample plot plant community types, based on moisture conditions, the presence or absence of *Sphagnum* moss on the peat surface, and the field layer vegetation, including *C. vulgaris*, *Carex rostrata* (Stokes), and *E. vaginatum* (Fig. 1).

The sample plot measurements of net ecosystem exchange (NEE) and methane (CH_4) fluxes were adjusted based on the surface area covered by different plant community types (PCTs) at each site. Since the 10 gas flux sample plots per site did not encompass all PCT and treatment combinations, the following adjustments were made:

Gas flux means for each Plant Community Type (PCT) were calculated using the sample plots available within each site, considering both the PCT and the treatment. In cases where certain PCT and treatment combinations were not present in the site's sample plots, adjustments were made by using mean values from similar sites. For "wet" sites, the data from Hoikkasuolenneva, Kivisalmenneva South, Kivisalmenneva North, Liminganneva, and Nimetonneva were applied, while for "dry" sites, the mean values from Peurainneva, Tuuraneva, and Ylimysneva were used. When handling treatment specific PCTs across sites, such as bare peat dominated or Eriophorum dominated in harvested areas and Ombrotrophic high lawn in control areas, the means were applied to the corresponding treatments. If a sample plot with the PCT "Bare peat dominated" was missing in the control treatment area, the corresponding plot from the harvested area was used. In cases where such data were unavailable, mean values from the wet or dry site categories were applied. Additionally, areas impacted by harvesting machinery routes were treated as harvested areas to ensure comprehensive coverage of vegetation disturbances caused by harvesting activities.

Finally, the total greenhouse gas C budget (GGCB, gC $m^{-2}yr^{-1}$), that shows the net gaseous C intake/uptake rate in the ecosystem was calculated from surface weighted seasonal and annual values as follows:

$$GGCBseasonal = NEEseasonal - F_{CH4seasonal} \quad (5)$$

$$GGCBannual = NEEseasonal - (Rseasonal*0.15) - F_{CH4} \quad (6)$$

The $NEE_{seasonal}$ covers both average cumulative gross primary production (g C $m^{-2}yr^{-1}$), and average cumulative ecosystem respiration (g

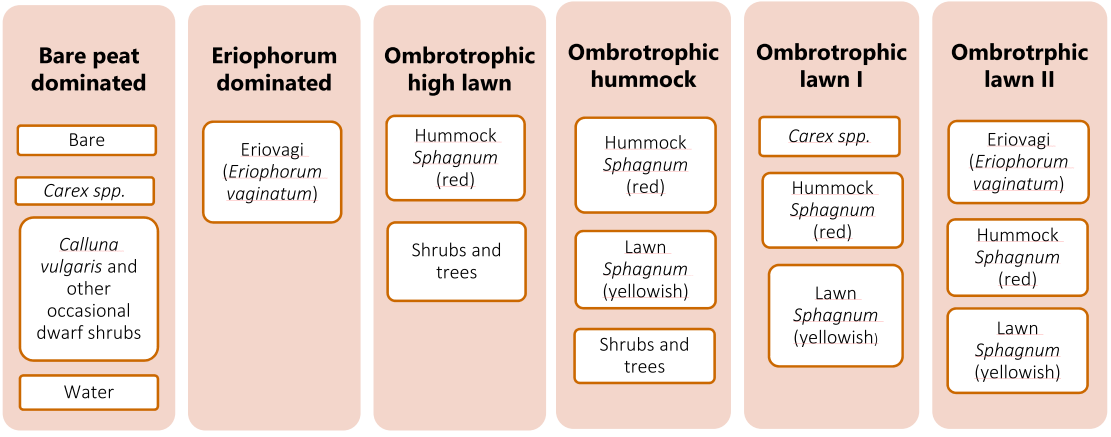

Fig. 1. Sample plot vegetation types (Plant Community Types, PCT) matched with vegetation types obtained through aerial imaging and random forest supervised classification. Vegetation types (PCT) are highlighted in bold for clarity.

C $m^{-2}yr^{-1}$). FCH4seasonal is the average cumulative emission of CH_4 (g C $m^{-2}yr^{-1}$). For the months, November–March, when measurements were not done, 15% was added to $CH_{4seasonal}$ C exchange and 15% of seasonal Re was added added to $NEE_{seasonal}$ to calculate annual values.

3. Results

3.1. Vegetation characteristics

T-SNE -clustering resulted in six visually and ecologically distinct plant community types (PCTs), comprising of bare peat dominated, *Eriophorum* dominated, Ombrotrophic hummock, Ombrotrophic high lawn and two Ombrotrophic lawn types (Fig. 2A). The names were given to represent the microtopographical variation in vegetation, or in case of sparse vegetation, according to the dominating plant species. T-SNE was found particularly well-suited for clustering tasks, as it aims to separate data points into distinct clusters based on their similarities. This clustering capability of t-SNE can lead to more accurate and visually distinct cluster representations compared to NMDS. The NMDS configuration, in this case, with a stress value of 0.169, captured the underlying dissimilarities in the data fairly well, but not as well as t-SNE. This resulted in clusters combining bare peat sample plots with 0% vegetation and ombrotrophic lawn vegetation combined with ombrotrophic hummocks with 100% vegetation cover (Fig. 2B). The weaker ability of NMDS to detect dissimilarities was also evident in the centroid crowding of the PCT and treatment combinations.

Vegetation of the harvested and control areas varied from each other (Mantel test on Bray-Curtis dissimilarity matrices shows no correlation, $p = 0.93$, 10,000 permutations), and the harvested areas were impacted by the time elapsed since harvesting (permutation ANOVA via adonis2 function from R package "vegan" on Bray-Curtis dissimilarity matrices for groups by years after harvest, $p = 0.0002$, 10,000 permutations). The bare peat dominated and the *Eriophorum* dominated sample plots were present only in the harvested areas, while the Ombrotrophic hummock and Ombrotrophic lawn I and II plant community types had sample plots in both harvested and control areas. The aerial image analysis, however, showed that the two sample plots classified as Ombrotrophic hummock types and three sample plots classified as Ombrotrophic lawn I and II types in the harvested areas were located on the harvesting machinery route and not in the actual harvested area. The Ombrotrophic lawn type I and II sample plots in the actual harvested areas, which most closely resembled the original vegetation type, were located in the older harvested sites. Some bare peat dominated PCTs in harvested areas began to resemble *Eriophorum* dominated PCTs in the second measuring year, indicating vegetation succession.

The observed plant species were common to nutrient poor oligo- and ombrotrophic peatlands (Table 2). The total vegetation cover was highest at the Ombrotrophic hummock and Ombrotrophic lawn II and I sample plots at the harvested areas. Graminoids were more abundant at the harvested plots (pooled graminoids difference between means 15.4% permutation test $p = 0.014$. $n = 40$), while shrubs were more abundant at the control plots (pooled shrubs difference between means −13.6% permutation test $p = 1e\text{-}5$. $n = 40$). While Ombrotrophic hummock and the two Ombrotrophic lawn PCT's had the highest coverage of *Sphagnum* mosses at harvested areas, it was still lower than the *Sphagnum* cover of the two ombrotrophic lawn types at the control area (difference between means −18.2%, permutation test $p = 0.0412$) (Table 2).

At site level, the cover of PCT's varied based on the harvesting age. The young sites harvested 1–2 years ago had large cover, 90–100%, of bare peat surface, while *Eriophorum* dominated surfaces had started to expand relatively quickly, with the older harvesting sites having 7–49% of area covered by *Eriophorum* dominated vegetation (Fig. 3). This early successional vegetation type was not typical in the control areas. *Sphagnum* covered areas were sparse (<20%) in all harvested areas, existing mainly as PCTs Ombrotrophic lawn I and II that had 86% and 57% *Sphagnum* cover (Table 2). The PCTs most typical for control areas, namely Ombrotrophic lawns, high lawns and hummocks still had rather low areal coverage even in the 5–7 years ago harvested sites (Fig. 3). There was no clear pattern in the increase of areal coverage for moss dominated PCTs (Ombrotrophic Hummock, and Ombrotrophic Lawns I and II) in older sites (4–7 years post-harvest). Notably, two sites showed less than 5% coverage of moss dominated PCTs, while the remaining three sites ranged from 15% to 40% coverage (Fig. 3).

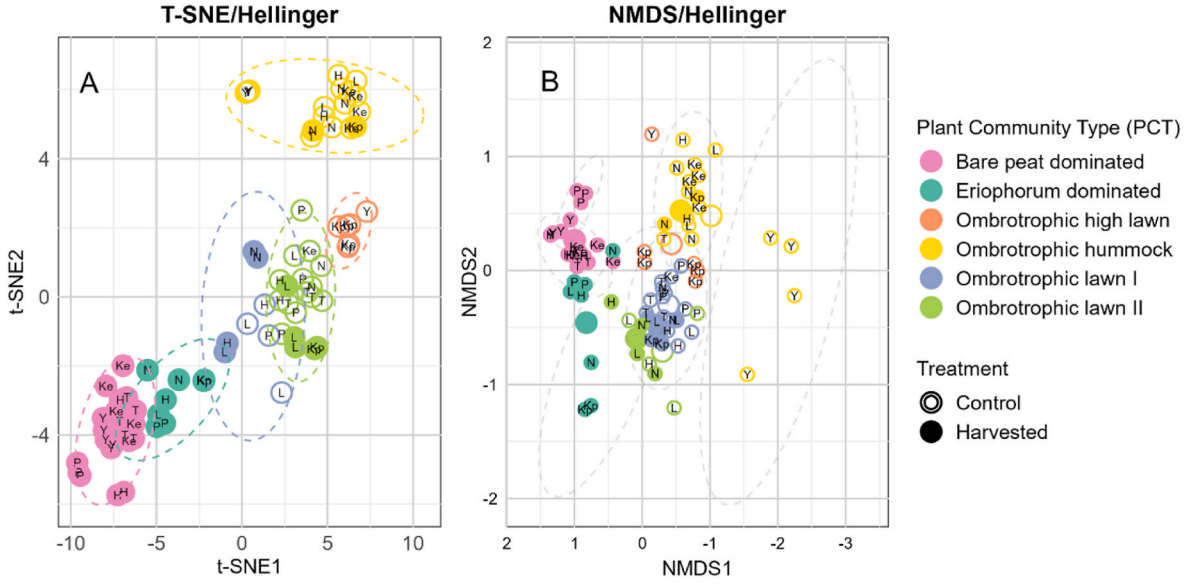

Fig. 2. A) t-distributed stochastic neighbor embedding (t-SNE) plot of the measured sample plots and their clusters based on Plant community type (PCT) and Treatment. Each dotted line in the t-SNE plot showcases distinct cluster within a reduced and scaled feature space derived from autoencoder embedding. B) Non-metric multidimensional scaling (NMDS) clustering of the measured sample plots. The sample plot colors and shapes are same as in the t-SNE clustering and gray dotted ellipses represent the NMDS clustering. The big circles in the NMDS plot represent geometric center (centroids) of the PCT and Treatment combination. The treatments are control, that represent sample plots with original vegetation and harvested, that represent the sample plots in the harvested area. Letters represent sites: Y = Ylimysneva, KE = Kivisalmenneva south, T = Tuuraneva, L = Liminganneva, KP = Kivisalmenneva north, P = Peurainneva, H = Hoikkasuolenneva and N = Nimetonneva. (For interpretation of the references to color in this figure legend, the reader is referred to the Web version of this article.)

Table 2
Plant community type characteristics (PCT), described by treatment, number of sample plots (n), and the most common plant species and the % cover of most abundant plant groups (*Sphagnum* mosses, graminoids and shrubs) measured in June/July 2022.

PCT	Treatment	n	Dominant species	Mean bare peat cover (%)	Mean *Sphagnum* cover (%)	Mean Graminoids cover (%)	Mean Shrubs cover (%)
Bare peat dominated	harvested	21	Mosses: *Sphagnum angustifolium* (C.E.O. Jensen ex Russow) and *Polytrichtum strictum* (Brid.) Vascular plants: *Calluna vulgaris* and *Carex rostrata*	92	2	3	7
Eriophorum dominated	harvested	8	Mosses: *Sphagnum angustifolium* and *Sphagnum fuscum*. (Schimp.) Vascular plants: *Eriophorum vaginatum* and *Calluna vulgaris*	54	2	65	3
Ombrotrophic hummock	harvested	2	Mosses: *Sphagnum fuscum* and *Sphagnum angustifolium* Vascular plants: *Empetrum nigrum* (L.) and *Calluna vulgaris*	2	90	1	52
Ombrotrophic lawn I	harvested	5	Mosses: *Sphagnum angustifolium* and *Sphagnum medium* (Limpr.) Vascular plants: *Carex rostrata* and *Calluna vulgaris*	4	86	6	3
Ombrotrophic lawn II	harvested	4	Mosses: *Sphagnum angustifolium* and *Sphagnum medium* Vascular plants: *Eriophorum vaginatum* and *Vaccinium oxycoccos* (L.)	17	57	38	5
Ombrotrophic high lawn	control	6	Mosses: *Sphagnum angustifolium* and *Sphagnum capillifolium* (Ehrh.) Hedw. Vascular plants: *Empetrum nigrum* and *Rubus chamaemorus* (L.)	4	35	5	50
Ombrotrophic hummock	control	16	Mosses: *Sphagnum fuscum* and *Pleurozium schreberi* (Willd. ex Brid.) Vascular plants: *Rubus chamaemorus* and *Empetrum nigrum*	0	73	1	24
Ombrotrophic lawn I	control	14	Mosses: *Sphagnum angustifolium* and *Sphagnum fuscum* Vascular plants: *Empetrum nigrum* and *Calluna vulgaris*	2	97	6	17
Ombrotrophic lawn II	control	4	Mosses: *Sphagnum angustifolium* and *Sphagnum papillosum* (Lindb.) Vascular plants: *Eriophorum vaginatum* and *Andromeda polifolia* (L.)	4	75	26	25

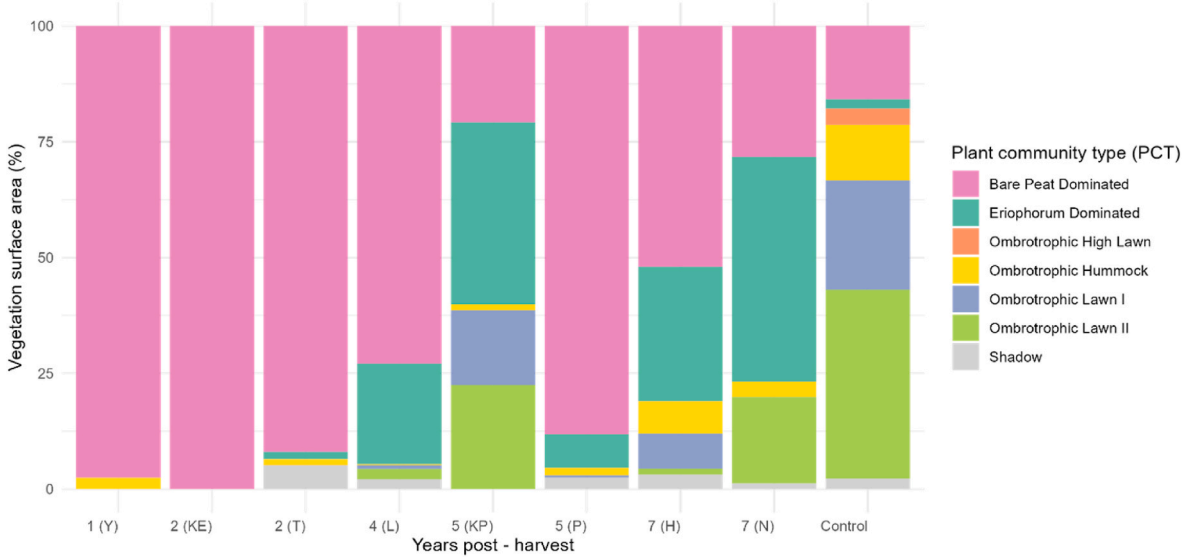

Fig. 3. Harvested areas vegetation cover percentage per site, retrieved from image data taken in June/July 2022. Letters represent sites: Y = Ylimysneva, KE = Kivisalmenneva south, T = Tuuraneva, L = Liminganneva, KP = Kivisalmenneva north, P = Peurainneva, H = Hoikkasuolenneva and N = Nimetonneva. It was not possible to determine the plant community type from the Shadow areas. All control sites are shown together.

3.2. Seasonal development of sample plot greenness and water table level

Green chromatic coordinate values (GCC), that in this study represent the photosynthetically active leaf area in the sample plots, were highest in sites harvested 4–5 years earlier in both years 2022 and 2023, and lowest in youngest harvested areas, 1–2 years post-harvest (Fig. 5). In older harvested sites GCC was the same or slightly higher and on younger harvested areas lower when compared to the control areas. In both study years greenness peak was seen in July in the control areas and in August in the harvested areas.

Of the measured sample plot PCTs, sample plots at harvested areas were similarly wet, with Ombrotrophic lawn I on average, but not significantly, the wettest, whereas Ombrotrophic high lawn and High hummock sample plots at control areas were the dryest (difference of means −10.3 cm, permutation-ANOVA with F-statistic $p < 0.0001$, n = 25 in high lawn and hummock PCTs, and n = 36 in lawn I and II). In general, all the PCTs that were present in both harvested and control areas had higher water table levels in harvested areas in both years. The water table levels were altogether higher in the year 2023, that can be explained partly by the higher precipitation in the previous winter months. Generally, at the site level, the water table levels (WTLs) were the same or higher in harvested areas compared to control areas (permutation tests: site H mean difference 18.2 cm p = 0.0026, site KE mean difference 24.9 p = 2e-5, site KP mean difference 22.6 p = 1e-5, site L mean difference 14.0 p = 0.0007, site N mean difference 22.5 p = 0.0, site Y mean difference 10.7 p = 0.0049, site T difference not significant. n = 10), with one exception: at one site, 5–6 years post-harvest, the levels dropped below −60 cm (permutation test: site P mean difference −12.9 p = 0.0013. n = 10) (Fig. 4). Based on the water table level the harvested sites were classified as either dry (Peurainneva, Tuuraneva and Ylimysneva) or wet (Hoikkasuolenneva, Kivisalmenneva south, Kivisalmenneva north, Liminganneva and Nimetonneva). Water table levels were at their lowest in July in harvested and control areas in both measured years (Fig. 4).

3.3. GHG development over time since harvesting

The measured CH_4 fluxes varied from −9.7 to 88.1 mg m^{-2} h^{-1} on harvested areas and from −0.6 to 21.0 mg $m^{-2}h^{-1}$ on control areas at the two-year measuring period, and the treatment and the yearly fluxes differed (permutation-based ANOVA, 10,000 permutations, $p < 2.2e-16$ and p = 2e-04, respectively, Table S1.3). During dark measurements, the momentary ecosystem respiration (ER) ranged from −3.8 to 0.0 g CO_2 $m^{-2}h^{-1}$ in the harvested areas and from −5.1 to 0.0 g CO_2 $m^{-2}h^{-1}$ in control areas (Table S1.3). A significant difference was observed between treatments (permutation-based ANOVA, 10,000 permutations, p = 0.0334, Table S1.3but no significant difference was detected between years (permutation-based ANOVA, 10,000 permutations, p = 0.1401, Table S1.3). NEE values measured in moderate to high light range (350–1050 µmol$m^{-2}s^{-1}$, average sample point light saturation point being ~ 700 µmol $m^{-2}s^{-1}$ (Parameter α represents the half-saturation constant in the context of photosynthetic light-response curve, Table S1.1), ranged from −2.0 to 2.8 g CO_2 $m^{-2}h^{-1}$ in the harvested areas and from −1.5 to 2.2 g CO_2 $m^{-2}h^{-1}$ in the control areas, and the fluxes differed between the treatments and the years (permutation-based ANOVA, 10,000 permutations, p = 0.0062 and $p < 2.2e-16$, respectively, Table S1.3).

The seasonal surface area weighted CH_4 flux varied from 0.3 to 31.7 g CH_4 m^{-2} at the harvested sites and from 1.2 to 11.2 g CH_4 m^{-2} at the control areas. In harvested areas the methane fluxes were highest in sites where wet conditions and *Eriophorum* dominated vegetation coexisted (Table 2, Fig. 5). Fluxes were lowest in the dry bare peat dominated sites. CH_4 fluxes were generally lower in the year 2022 than in the year 2023.

The seasonal surface area weighted NEE varied from positive (CO_2 sink) to negative (CO_2 source) in both harvested areas and control areas (Fig. 5). In the harvested areas the highest CO_2 sources were the two young sites that still lacked vegetation. Correspondingly the gross primary production (GPP) at these sites was the lowest (Table 3). Highest NEE (CO_2 sink) of the harvested areas were observed at the "middle aged" sites (Fig. 5; Table 3) with the highest GCC throughout the seasons (Fig. 5). Highest ecosystem respiration (ER) rates (CO_2 source) of harvested sites were observed at dry sites where water table levels were consistently low (Fig. 5; Table 3). However, both the highest yearly NEE and the lowest yearly NEE was measured at the control areas (Table 3).

The youngest dry harvested areas (1–2 years post-harvest) were the highest sources of carbon to atmosphere, while the 4–5 years ago harvested wet sites were the greatest C sinks. In the oldest harvesting sites included in this study, the C budget was close to zero (Fig. 5 and Table 4). In addition, the C budget of control areas ranged from negative to positive, with the forestry drained sites being the highest carbon sources to atmosphere.

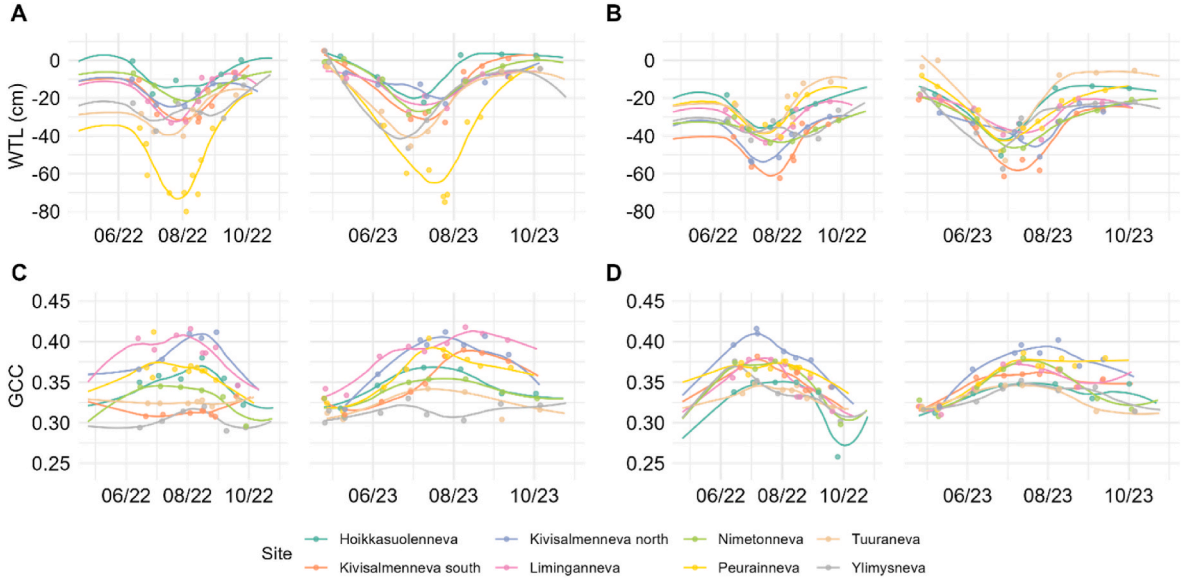

Fig. 4. Interpolated daily value lines combined with measured data mean points for the years 2022–2023. Panels A and C represent the harvested sample plots, while Panels B and D represent the control sample plots. The harvested plots are located in areas where vegetation was harvested, whereas the control plots consist of original, undisturbed vegetation. Lines are smoothed using a span of 0.4. The plots display water table levels (WTL) and green chromatic coordinate (GCC) values throughout the growing seasons from April 24 to October 30, covering a period of 184 days. Detailed measured means and standard deviations (SD) for WTL and GCC are provided in the supplementary information, Table S1.3. (For interpretation of the references to color in this figure legend, the reader is referred to the Web version of this article.)

Table 3
Plant community type specific sample plot water table level (WTL) seasonal average (±SE, ±SD) measured during growing seasons 2022–2023.

PCT	Treatment	n	Mean WTL cm	
			2022	2023
Bare peat dominated	harvested	21	−27 se ± 1.3 sd ± 25.6	−19 se ± 0.9 sd ± 24.6
Eriophorum dominated	harvested	8	−22 se ± 1.4 sd ± 21.6	−16 se ± 1.3 sd ± 22.5
Ombrotrophic hummock	harvested	2	−21 se ± 1.3 sd ± 8.1	−17 se ± 1.2 sd ± 10.2
Ombrotrophic lawn I	harvested	5	−15 se ± 0.9 sd ± 11.6	−10 se ± 0.9 sd ± 11.8
Ombrotrophic lawn II	harvested	4	−21 se ± 0.8 sd ± 9.1	−19 se ± 1.4 sd ± 16.8
Ombrotrophic high lawn	control	6	−39 se ± 0.9 sd ± 10.5	−33 se ± 0.8 sd ± 11.2
Ombrotrophic hummock	control	16	−39 se ± 0.6 sd ± 12.1	−34 se ± 0.6 sd ± 14.9
Ombrotrophic lawn I	control	14	−25 se ± 0.8 sd ± 11.5	−22 se ± 0.8 sd ± 13.4
Ombrotrophic lawn II	control	4	−26 se ± 0.7 sd ± 11.1	−22 se ± 0.9 sd ± 15.7

4. Discussion

This study shows that the initial development of vegetation and correspondingly net CO_2 exchange and CH_4 emissions following *Sphagnum* moss harvesting depends largely on the peatland moisture conditions. Dry conditions lead to dominance by bare peat with sparse ericoid shrub vegetation, while wet conditions result in *E. vaginatum* dominance. As hypothesized gas fluxes closely follow the changes in vegetation composition.

4.1. Vegetation development on Sphagnum harvested sites

The underlying expectation of *Sphagnum* moss harvesting is that the moss is renewable, allowing for repeated harvesting at the same sites after a certain period. However, based on the results obtained, *Sphagnum* spontaneous self-regeneration is a very slow process. Significant variation in *Sphagnum* moss regeneration was observed between wet strip-harvested sites, where coverage ranged from 2% to 28%, and dry clear-harvested sites, where it was almost entirely absent. Although some gas flux sample plots in older strip-harvested sites exhibited notably higher *Sphagnum* cover, reaching up to 95%, analysis of aerial images indicated that these plots were located between harvested strips and were used as access tracks for harvesting machinery. Thus, the presence of *Sphagnum* moss was not due to regeneration but rather a result of its retention through the harvesting process. The findings align with studies from abandoned peat extraction areas, where *Sphagnum* moss coverage of up to 21% has been observed in the best cases (Lavoie et al., 2005b; Poulin et al., 2005; Triisberg et al., 2011). This contrasts sharply with findings from Canadian “donor sites,” where complete recovery of *Sphagnum* cover was observed within 11 years following the harvesting of the top 10 cm of the peatland surface (Guêné-Nanchen et al., 2019). The difference in harvesting methods, particularly the depth of harvesting, appears to be crucial for recovery.

After harvesting, vegetation development is influenced by the hydrological conditions. In wet sites, pioneer species commonly associated with bare peat surfaces, such as *E. vaginatum* (Tuittila et al., 2000; Campbell et al., 2003; Rochefort et al., 2013), established quickly and dominated the older sites (4–7 years post-harvest). The duration of our study was insufficient to observe the often-reported decline in *E. vaginatum* cover, which typically facilitates the establishment of other peatland species (Lavoie et al., 2005a; Rochefort et al., 2013). For example, the cover of shrubs was very low in our study sites. Ericaceous shrubs are known to require a longer time for establishment (Pouliot et al., 2011), and similar cover levels to those observed in our control sites have been reported in studies spanning over 20 years (Poulin et al., 2005). As *E. vaginatum* is recognized for its role in facilitating *Sphagnum* regeneration (Tuittila et al., 2000), it is possible that *Sphagnum* establishment may occur in the long term. However, after the first seven years, the results are not very promising. if associated with Canadian restoration sites, our sites would be classified in the least successful category of "Low cover-diverse peatland plant," indicating that the restoration efforts have not succeeded (González et al., 2013, 2014).

In the dry sites the vegetation development took a different direction as still five years since harvesting the bare peat surfaces dominated the site, with ericoid dwarf-shrub *C. vulgaris* being the most common species. Similar low self-revegetation has been found to be a common feature in abandoned peat extraction areas as dryness (water table level <40 cm), frost, high temperatures on bare peat surface and destroyed propagule banks and peat chemistry make it difficult for germination and survival of seedlings (Poulin et al., 2005; Triisberg et al., 2013; Vozbrannaya et al., 2022).

4.1.1. GHG exchange in wet sites

As hypothesized, the greenhouse gas (GHG) exchange closely followed the development of vegetation composition. In our wet young sites, the combination of water table level fluctuations, and sparse or absent vegetation—i.e., minimal substrate for methanogens—resulted in low CH_4 emissions. Under these relatively wet conditions, the gross photosynthesis of the sparse vegetation (*E. vaginatum*) was sufficient to counterbalance peat decomposition, leading to net CO_2 uptake and, due to the relatively low CH_4 emissions, also to gaseous carbon uptake.

The rapid increase in *E. vaginatum* cover after harvesting significantly influenced both CH_4 and CO_2 gas exchange. The highest methane emissions were observed at the wet, *E. vaginatum*-dominated site 4–6 years post-harvest, being tenfold higher compared to control areas. The aerenchymatous tissue of *E. vaginatum* efficiently transports methane from the peat to the atmosphere (Lai et al., 2014) and additionally produces photosynthates released as root exudates into the rhizosphere, thereby providing fresh substrate for methanogens and inducing methane production (Dorodnikov et al., 2011). Along with high methane emissions, the rapid growth of new *E. vaginatum* leaves and its capacity for CO_2 sequestration under high light conditions (light saturation point at ~1200 μmol m^2 s^{-1}; Robertson and Woolhouse, 1984) led to high gross primary production. Coupled with modest respiration, this resulted in a strong net CO_2 and gaseous carbon sink. Similar observations have been made in other studies, where *E. vaginatum* played a crucial role in high rates of CO_2 uptake following restoration (Tuittila et al., 1999).

In the oldest harvesting sites, characterized by more patterned surfaces with mixed vegetation communities, methane emissions remained high, but net CO_2 exchange hovered around zero. The methane emissions from the wet harvested sites are more comparable to those observed in minerotrophic mires than in ombrotrophic mires (Saarnio et al., 2009). It has been noted that CH_4 emissions decrease with an abundant *Sphagnum* layer due to methane-oxidizing bacteria (methanotrophs, MOB), which inhabit the dead, water-filled hyaline cells of *Sphagnum* and provide the plant with CO_2 derived from CH_4 oxidation (Putkinen et al., 2018). However, such dense *Sphagnum* layer is mostly still missing from the harvesting sites. The measured net ecosystem exchange (NEE) values in our study showed similar tendencies as those reported by Aurela et al. (2007) from an oligotrophic poor fen. The comparable vegetation types, namely bare peat-dominated sample plots

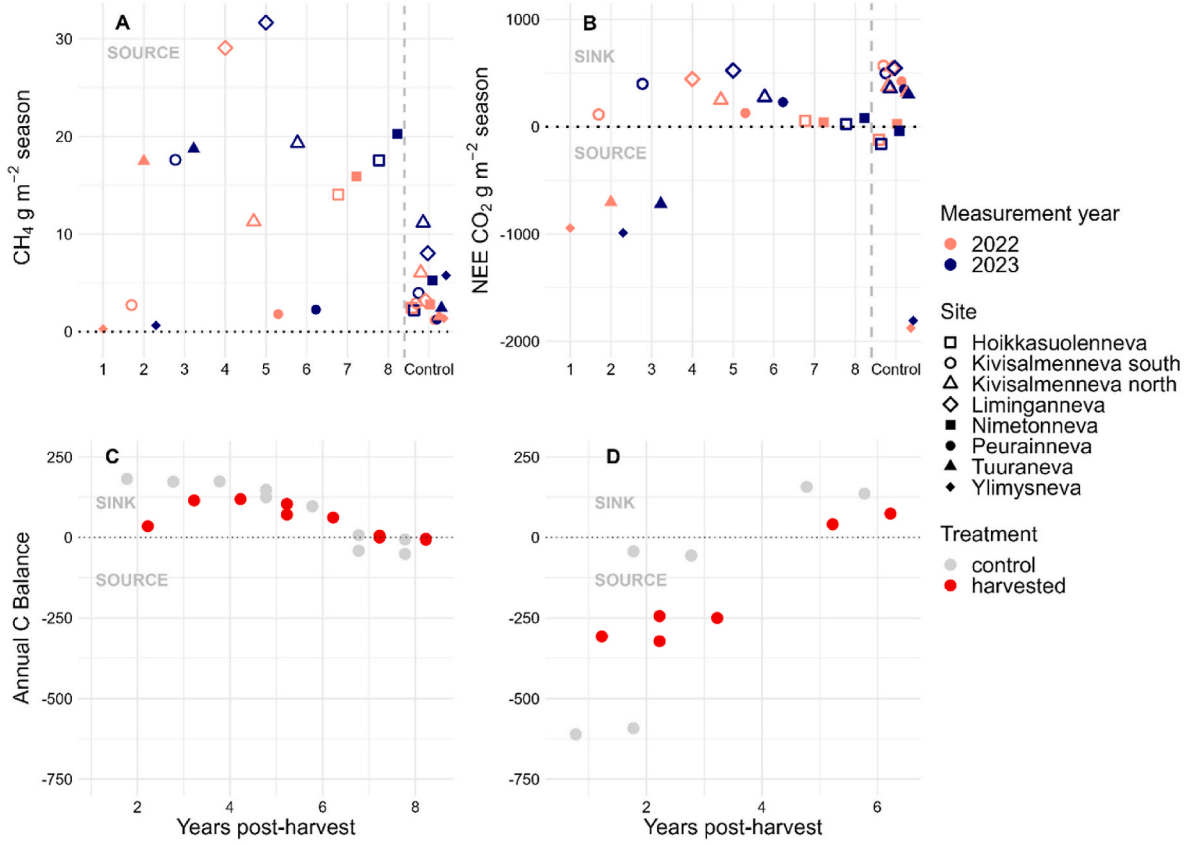

Fig. 5. Seasonal cumulative surface area weighted A) methane (CH_4) and A) net ecosystem CO_2 exchange (NEE) fluxes from 1 to 8 years ago harvested sites measured in 2022 and 2023. Growing season in both years 24. Of April – 30. October, 184 days. Positive NEE values indicate the ecosystem's uptake of CO_2 from the atmosphere, while negative NEE values indicate the emissions of CO_2 from the ecosystem to the atmosphere. Positive CH_4 values represent emissions to the atmosphere. Annual carbon (C) balance on C) wet and D) dry moisture conditions sites, calculated based on the amount of carbon in CO_2 and CH_4. Positive carbon balance values represent ecosystem carbon C uptake and negative value C emissions to the atmosphere. Wet peatland sites are Kivisalmenneva south, Liminganneva, Kivisalmenneva north, Hoikkasuolenneva and Nimetonneva. Dry peatland sites are Ylimysneva, Tuuraneva and Peurainneva. The treatments are control, that represent original vegetation and harvested, that represent the area where *Sphagnum* moss has been harvested.

without any vegetation and the control areas, had CO_2 flux ranges (~0–0.5 g CO_2 m^{-2} h^{-1} and -1–1 g CO_2 m^{-2} h^{-1}, respectively) similar to those reported by Aurela et al. (2007). The decrease in NEE (sink) observed in this study has also been documented during natural vegetation succession (Leppälä et al., 2008) and following restoration (Yli-Petäys et al., 2007), and has been linked to decreases in herb and/or graminoid cover. Conversely, the coexistence of herb/graminoid plants and *Sphagnum* mosses has been observed to increase CO_2 uptake (Kivimäki et al., 2008).

4.1.2. GHG exchange in dry sites

During the first years, post-harvest, the dry sites with little or no vegetation cover experienced drastic water table fluctuations due to the absence of capillary water transport by *Sphagnum* mosses. This led to water table drawdown and crust formation during dry periods and flooding during rainy periods (McNeil and Waddington, 2003). The greenhouse gas (GHG) exchange at the three harvested dry sites varied. Two of these sites (the youngest and oldest) exhibited very low CH_4 emissions, aligning general understanding that a lack of vegetation and lower water tables suppress anoxic methanogenic activity (Tian et al., 2023). However, one site supported high methane emissions due to two out of five sample plots located in a depression within the peatland. When the depression was waterlogged and devoid of *Sphagnum*-associated methanotrophs consuming the CH_4 (van Winden et al., 2012), high levels of methane were emitted even when *E. vaginatum* vegetation was still sparse (Wilson et al., 2009).

As anticipated, in the first years following harvest, the dry sites functioned as net sources of CO_2 due to lower photosynthetic activity, which was insufficient to offset the CO_2 released from peat decomposition. This finding is consistent with earlier studies from abandoned peat extraction sites (Waddington and McNeil, 2002; Strack and Zuback, 2013; Nugent et al., 2021). Surprisingly, the older dry site, characterized by the lowest water table and a surface mainly covered by bare peat with sparse *C. vulgaris* and *E. vaginatum* vegetation, was a CO_2 sink. Due to the expectation of high peat decomposition under such conditions, the high carbon binding ability of this vegetation type was unexpected. One potential explanation could be related to the composition and activity of the soil microbial community associated with *C. vulgaris*. *C. vulgaris* is known to be associated with *Ericoid Mycorrhiza* (ErM), and the mutualistic relationship between the plant and the fungi has been shown to enhance plant growth rate, rooting of propagules, drought tolerance, and promote higher net photosynthetic and transpiration rates (Shao et al., 2022; Wei et al., 2022).

4.1.3. GHG exchange in control sites

Similar to harvested sites, also the control areas varied in their GHG exchange. As all the sites were relatively dry and nutrient poor, supporting mainly *Sphagnum* moss dominated high lawn/hummock plant communities the methane emissions were low and in similar range as has been measured from undrained and drained nutrient poor peatlands (Rinne et al., 2007; Jackowicz-Korczyński et al., 2010; Riutta et al., 2020). The net CO_2 exchange of the control sites varied greatly according to their land use intensity and highest annual CO_2 emissions were observed from the forestry drained control sites.

Table 4
Modelled seasonal methane (g CH_4 m^{-2}), gross primary production (GPP, g CO_2 m^{-2}), ecosystem respiration (R, g CO_2 m^{-2}), net ecosystem exchange (NEE, g CO_2 m^{-2}), greenhouse gas C budget (GGCB, g C m^{-2}) and annual methane (g CH_4 m^{-2}), net ecosystem exchange (NEE, g CO_2 m^{-2}), and greenhouse gas C budget (GGCB, g C m^{-2}). From newest harvested to oldest harvested from left to right. Positive NEE and GPP values indicate the ecosystem's uptake of CO_2 from the atmosphere, while negative NEE and ER values indicate the emissions of CO_2 from the ecosystem to the atmosphere. Positive GGCB values represent ecosystem carbon C uptake and negative value C emissions to the atmosphere. Positive CH_4 values represent emissions to the atmosphere. **Emissions to the atmosphere are bolded**. The treatments are control, that represent original vegetation and harvested, that represent the area where *Sphagnum* moss has been harvested.

Site	Y	KS	T	L	KN	P	H	N
Moisture conditions	dry	wet	dry	wet	wet	dry	wet	wet
Years post-harvest	1–2	2–3	2–3	4–5	5–6	5–6	7–8	7–8
Harvested								
CH_4 seasonal								
2022	**0**	**3**	**18**	**29**	**11**	**2**	**14**	**16**
2023	**1**	**18**	**19**	**32**	**19**	**2**	**18**	**20**
GPP seasonal								
2022	478	872	680	1400	1487	1716	1446	1137
2023	528	1375	715	1354	1468	1706	1480	1167
ER seasonal								
2022	**−1422**	**−759**	**−1348**	**−956**	**−1237**	**−1583**	**−1389**	**−1094**
2023	**−1516**	**−975**	**−1434**	**−949**	**−1226**	**−1472**	**−1446**	**−1133**
NEE seasonal								
2022	**−944**	114	**−704**	444	250	132	57	43
2023	**−988**	400	**−719**	404	242	234	34	33
CH_4 annual								
2022	**0**	**3**	**20**	**33**	**13**	**2**	**16**	**18**
2023	**0.74**	**20.25**	**21.53**	**36.42**	**22.22**	**2.60**	**20.19**	**23.30**
NEE annual								
2022	**−1157**	0	**−911**	301	64	**−105**	**−151**	**−121**
2023	**−1216**	253	**−934**	262	58	13	**−183**	**−137**
GGCB seasonal								
2022	**−267**	30	**−212**	104	62	36	6	0
2023	**−280**	100	**−217**	91	54	64	**−4**	**−6**
GGCB annual								
2022	**−307**	25	**−244**	82	50	30	2	**−3**
2023	**−322**	81	**−250**	70	41	54	**−4**	**−7**
Control								
CH_4 seasonal								
2022	**1**	**3**	**2**	**3**	**6**	**1**	**2**	**3**
2023	**6**	**4**	**2**	**8**	**11**	**1**	**2**	**5**
GPP seasonal								
2022	1036	1618	1167	1684	1702	2037	1007	1862
2023	837	1556	1145	1569	1576	1960	1062	1762
ER seasonal								
2022	**−2912**	**−1049**	**−1295**	**−1139**	**−1301**	**−1551**	**−1127**	**−1833**
2023	**−2643**	**−1013**	**−1311**	**−1091**	**−1248**	**−1538**	**−1212**	**−1766**
NEE seasonal								
2022	**−1876**	569	**−128**	545	400	486	**−120**	29
2023	**−1806**	543	**−166**	478	327	423	**−150**	**−4**
CH_4 annual								
2022	**2**	**3**	**2**	**4**	**7**	**1**	**3**	**3**
2023	**7**	**5**	**3**	**9**	**13**	**1**	**3**	**6**
NEE annual								
2022	**−2313**	411	**−322**	374	205	253	**−289**	**−246**
2023	**−2202**	391	**−363**	314	140	192	**−332**	**−269**
GGCB seasonal								
2022	**−531**	159	**−37**	152	109	137	**−36**	6
2023	**−515**	150	**−49**	129	84	119	**−44**	**−5**
GGCB annual								
2022	**−611**	134	**−43**	128	91	116	**−41**	5
2023	**−592**	127	**−56**	108	69	100	**−51**	**−6**

4.1.4. Climate forcing

In evaluating the impacts of *Sphagnum* moss harvesting on greenhouse gas (GHG) emissions, it is crucial to consider the net effects on climate forcing. Preliminary findings indicate that while harvesting may lead to temporary increases in CO_2 uptake, it is also associated with elevated emissions of methane. This duality underscores the complexity of the environmental impacts of moss harvesting practices and highlights the need for a comprehensive assessment of these competing dynamics to fully understand their implications.

5. Conclusions

While the assumption of sustainable *Sphagnum* harvesting is based on the renewability of the harvested material, our study indicates that the process is likely slower than anticipated and heavily dependent on the hydrological conditions that develop at the sites post-harvest. *Sphagnum* moss regeneration seems unlikely at dry sites and is clearly slower at wet sites compared to cutover peatlands restored using the moss layer transfer technique. Without renewal measures such as rewetting and replanting, delays in vegetation re-establishment are expected.

The CO_2 and methane exchange is highly dependent on vegetation

succession but appears to develop to a level that resembles that of undrained control sites within 5–7 years post-harvest, despite differences in vegetation composition. Particularly at wet sites, the successional stage 4–6 years after harvesting, characterized by wet, *Eriophorum* dominated vegetation, was a strong CO_2 sink. Despite high CH_4 emissions, these sites formed a gaseous carbon sink from the atmosphere.

Future research should focus on long-term monitoring of vegetation recovery and related functions to determine the actual rotation time of *Sphagnum* harvesting. Additionally, management practices should be developed to enhance *Sphagnum* regeneration at harvesting sites. Understanding the ecohydrological feedback in these ecosystems will be crucial for optimizing the climate impact of the produced growing media.

CRediT authorship contribution statement

Satu K. Karjalainen: Writing – original draft, Visualization, Methodology, Investigation, Formal analysis, Data curation. **Jani Anttila:** Writing – review & editing, Supervision, Software, Methodology, Formal analysis, Data curation. **Liisa Maanavilja:** Writing – review & editing, Methodology, Investigation. **Alireza Hamedianfar:** Writing – review & editing, Methodology. **Anna M. Laine:** Writing – review & editing, Validation, Supervision, Project administration, Funding acquisition, Conceptualization.

Declaration of competing interest

The authors declare the following financial interests/personal relationships which may be considered as potential competing interests: Anna Laine reports financial support was provided by Finnish Ministry of Agriculture and Forestry. Jani Anttila reports financial support was provided by Finnish Ministry of Agriculture and Forestry. If there are other authors, they declare that they have no known competing financial interests or personal relationships that could have appeared to influence the work reported in this paper.

Acknowledgements

Financial support was provided through the Catch the Carbon project funded by the Ministry of Agriculture and Forestry Finland. We thank Pasi Arkko, Hanna Kenttä, Susanna Laukkakoski, Sanni Pälsi, Sanni Rantanen and Petri Salovaara who assisted with field surveys and managing of the survey equipment. A special thanks to Aino Korrensalo, Lauri Mehtätalo and Päivi Mäkiranta for sharing their expertise.

Appendix A. Supplementary data

Supplementary data to this article can be found online at https://doi.org/10.1016/j.jenvman.2024.123357.

Data availability

Data will be made available on request.

References

Alm, J., Shurpali, N., Tuittila, E.-S., Laurila, T., Maljanen, M., Saarnio, S., Minkkinen, K., 2007. Methods for determining emission factors for the use of peat and peatlands - flux measurements and modelling. Boreal Environ. Res. 12, 85–100.

Anderson, R., Bayer, P.E., Edwards, D., 2020. Climate change and the need for agricultural adaptation. Curr. Opin. Plant Biol. 56, 197–202. https://doi.org/10.1016/j.pbi.2019.12.006.

Aurela, M., Riutta, T., Laurila, T., Tuovinen, J.P., Vesala, T., Tuittila, E.S., Rinne, J., Haapanala, S., Laine, J., 2007. CO_2 exchange of a sedge fen in southern Finland-the impact of a drought period. Tellus B: Chem. Phys. Meteorol. 59 (5), 826–837. https://doi.org/10.1111/j.1600-0889.2007.00309.x.

Campbell, D.R., Rochefort, L., Lavoie, C., 2003. Determining the immigration potential of plants colonizing disturbed environments: the case of milled peatlands in Quebec. J. Appl. Ecol. 40 (1), 78–91. https://doi.org/10.1046/j.1365-2664.2003.00782.x.

Dorodnikov, M., Knorr, K.-H., Kuzyakov, Y., Wilmking, M., 2011. Plant-mediated CH4 transport and contribution of photosynthates to methanogenesis at a boreal mire: a 14C pulse-labeling study. Biogeosciences 8 (8), 2365–2375. https://doi.org/10.5194/bg-8-2365-2011.

Fritz, C., Pancotto, V.A., Elzenga, J.T.M., Visser, E.J.W., Grootjans, A.P., Pol, A., Iturraspe, R., Roelofs, J.G.M., Smolders, A.J.P., 2011. Zero methane emission bogs: extreme rhizosphere oxygenation by cushion plants in Patagonia. New Phytol. 190 (2), 398–408. https://doi.org/10.1111/j.1469-8137.2010.03604.x.

González, E., Rochefort, L., 2014. Drivers of success in 53 cutover bogs restored by a moss layer transfer technique. Ecol. Eng. 68, 279–290. https://doi.org/10.1016/j.ecoleng.2014.03.051.

González, E., Rochefort, L., Boudreau, S., Hugron, S., Poulin, M., 2013. Can indicator species predict restoration outcomes early in the monitoring process? a case study with peatlands. Ecol. Indicat. 32, 232–238. https://doi.org/10.1016/j.ecolind.2013.03.019.

González-Sargas, E., Rochefort, L., 2019. Declaring success in Sphagnum peatland restoration: identifying outcomes from readily measurable vegetation descriptors. Mires Peat 24. https://doi.org/10.19189/MaP.2017.OMB.305.

Greenup, A.L., Bradford, M.A., McNamara, N.P., Ineson, P., Lee, J.A., 2000. The role of Eriophorum vaginatum in CH4 flux from an ombrotrophic peatland. Plant Soil 227 (1), 265–272. https://doi.org/10.1023/A:1026573727311.

Gruda, N., 2019. Increasing sustainability of growing media constituents and stand-alone substrates in soilless culture systems. Agronomy 9 (6), 298. https://doi.org/10.3390/agronomy9060298.

Guêné-Nanchen, M., Hugron, S., Rochefort, L., 2019. Harvesting surface vegetation does not impede self-recovery of Sphagnum peatlands. Restor. Ecol. 27 (1), 178–188. https://doi.org/10.1111/rec.12834.

Jackowicz-Korczyński, M., Christensen, T.R., Bäckstrand, K., Crill, P., Friborg, T., Mastepanov, M., Ström, L., 2010. Annual cycle of methane emission from a subarctic peatland. J. Geophys. Res. Biogeosci. 115 (G2). https://doi.org/10.1029/2008JG000913.

Kitir, N., Yildirim, E., Şahin, Ü., Turan, M., Ekinci, M., Ors, S., Kul, R., Ünlü, H., Ünlü, H., 2018. Peat use in horticulture. In: Topcuoğlu, B., Turan, M. (Eds.), Peat. IntechOpen. https://doi.org/10.5772/intechopen.79171.

Kivimäki, S., Yli-Petays, M., Tuittila, E.-S., 2008. Carbon sink function of sedge and Sphagnum patches in a restored cut-away peatland. J. Appl. Ecol. 45, 921–929. https://doi.org/10.1111/j.1365-2664.2008.01458.x.

Korrensalo, A., Mehtätalo, L., Alekseychik, P., 2020a. Varying vegetation composition, respiration and photosynthesis decrease temporal variability of the CO2 sink in a boreal bog. Ecosystems 23, 842–858. https://doi.org/10.1007/s10021-019-00434-1.

Korrensalo, A., Mehtätalo, L., Alekseychik, P., Uljas, S., Mammarella, I., Vesala, T., Tuittila, E.-S., 2020b. Varying vegetation composition, respiration and photosynthesis decrease temporal variability of the CO2 sink in a boreal bog. Ecosystems 23 (4), 842–858. https://doi.org/10.1007/s10021-019-00434-1.

Kox, M.A.R., Smolders, A.J.P., Speth, D.R., Lamers, L.P.M., Camp, H.J.M.O. den, Jetten, M.S.M., van Kessel, M.A.H.J., 2021. A novel laboratory-scale mesocosm setup to study methane emission mitigation by Sphagnum mosses and associated methanotrophs. Front. Microbiol. 12. https://doi.org/10.3389/fmicb.2021.651103.

Kuiper, J.J., Mooij, W.M., Bragazza, L., Robroek, B.J.M., 2014. Plant functional types define magnitude of drought response in peatland CO 2 exchange. Ecology 95 (1), 123–131. https://doi.org/10.1890/13-0270.1.

Lai, D.Y.F., Moore, T.R., Roulet, N.T., 2014. Spatial and temporal variations of methane flux measured by autochambers in a temperate ombrotrophic peatland. Journal of Geophysical Research Biogeosciences 119 (5), 864–880. https://doi.org/10.1002/2013jg002410.

Laiho, R., Tuominen, S., Kojola, S., Penttilä, T., Saarinen, M., Ihalainen, A., 2016. Heikkotuottoiset ojitetut suometsät – missä ja paljonko niitä on? Metsätieteen Aikakauskirja 2016 (2). https://doi.org/10.14214/ma.5957.

Laine, A.M., Korrensalo, A., Tuittila, E.-S., 2019. Impacts of drainage, restoration and warming on boreal wetland greenhouse gas fluxes. Sci. Total Environ. 647, 169–181. https://doi.org/10.1016/j.scitotenv.2018.07.390.

Laine, A.M., Korrensalo, A., Tuittila, E.-S., 2022. Plant functional traits play the second fiddle to plant functional types in explaining peatland CO2 and CH4 gas exchange. Sci. Total Environ. 834, 155352. https://doi.org/10.1016/j.scitotenv.2022.155352.

Lavoie, C., Marcoux, K., Saint-Louis, A., Price, J.S., 2005a. The dynamics of a cottongrass (Eriophorum vaginatum L.) cover expansion in a vacuum-mined peatland, southern Québec, Canada. Wetlands 25 (1), 64–75. https://doi.org/10.1672/0277-5212(2005)025[0064:TDOACE]2.0.CO;2.

Lavoie, C., Saint-Louis, A., Lachance, D., 2005b. Vegetation dynamics on an abandoned vacuum-mined peatland: 5 Years of monitoring. Wetl. Ecol. Manag. 13 (6), 621–633. https://doi.org/10.1007/s11273-005-0126-1.

Leifeld, J., Wüst-Galley, C., Page, S., 2019. Intact and managed peatland soils as a source and sink of GHGs from 1850 to 2100. Nat. Clim. Change 9, 1–3. https://doi.org/10.1038/s41558-019-0615-5.

Leppälä, M., Kukko-Oja, K., Laine, J., Tuittila, E.-S., 2008. Seasonal dynamics of CO2 exchange during primary succession of boreal mires as controlled by phenology of plants. Ecoscience 15 (4), 460–471. https://doi.org/10.2980/15-4-3142.

Leppälä, M., Oksanen, J., Tuittila, E.-S., 2011. Methane flux dynamics during mire succession. Oecologia 165 (2), 489–499. http://www.jstor.org/stable/41500652.

Ma, N., Ide, S., Suematsu, K., Watanabe, K., Shimanoe, K., 2020. Novel solid electrolyte co2 gas sensors based on c-axis-oriented y-doped la9.66si5.3b0.7o26.14. ACS Applied Materials & Interfaces 12 (19), 21515–21520. https://doi.org/10.1021/acsami.0c00454.

McNeil, P., Waddington, J.M., 2003. Moisture controls on Sphagnum growth and CO 2 exchange on a cutover bog. J. Appl. Ecol. 40 (2), 354–367. https://doi.org/10.1046/j.1365-2664.2003.00790.x.
Nugent, K.A., Strachan, I.B., Strack, M., Roulet, N.T., Rochefort, L., 2018. Multi-year net ecosystem carbon balance of a restored peatland reveals a return to carbon sink. Global Change Biol. 24 (12), 5751–5768. https://doi.org/10.1111/gcb.14449.
Nugent, K.A., Strachan, I.B., Strack, M., Roulet, N.T., Ström, L., Chanton, J.P., 2021. Cutover peat limits methane production causing low emission at a restored peatland. J. Geophys. Res.: Biogeosciences 126 (12). https://doi.org/10.1029/2020JG005909.
Pedregosa, F., Varoquaux, G., Gramfort, A., Michel, V., Thirion, B., Grisel, O., Blondel, M., Müller, A., Nothman, J., Louppe, G., Prettenhofer, P., Weiss, R., Dubourg, V., Vanderplas, J., Passos, A., Cournapeau, D., Brucher, M., Perrot, M., Duchesnay, É., 2012. Scikit-learn: machine learning in Python. https://doi.org/10.48550/arXiv.1201.0490.
Peichl, M., Gažovič, M., Vermeij, I., de Goede, E., Sonnentag, O., Limpens, J., Nilsson, M. B., 2018. Peatland vegetation composition and phenology drive the seasonal trajectory of maximum gross primary production. Sci. Rep. 8 (1), 8012. https://doi.org/10.1038/s41598-018-26147-4.
Poulin, M., Rochefort, L., Quinty, F., Lavoie, C., 2005. Spontaneous revegetation of mined peatlands in eastern Canada. Can. J. Bot. 83 (5), 539–557. https://doi.org/10.1139/b05-025.
Pouliot, R., Rochefort, L., Karofeld, E., 2011. Initiation of microtopography in re-vegetated cutover peatlands: evolution of plant species composition. Appl. Veg. Sci. 15 (3), 369–382. https://doi.org/10.1111/j.1654-109x.2011.01164.x.
Putkinen, A., 2018. Sphagnum-associated methanotrophs – a resilient CH_4 biofilter in pristine and disturbed peatlands. Dissertationes Forestales (252). https://doi.org/10.14214/df.252.
Rinne, J., Riutta, T., Pihlatie, M., Aurela, M., Haapanala, S., Tuovinen, J.-P., Tuittila, E.-S., Vesala, T., 2007. Annual cycle of methane emission from a boreal fen measured by the eddy covariance technique. Tellus B 59 (3), 449. https://doi.org/10.1111/j.1600-0889.2007.00261.x.
Riutta, T., Korrensalo, A., Laine, A., Laine, J., Tuittila, E., 2020. Interacting effects of vegetation components and water level on methane dynamics in a boreal fen. Biogeosciences 17 (3), 727–740. https://doi.org/10.5194/bg-17-727-2020.
Robertson, K.P., Woolhouse, H.W., 1984. Studies of the seasonal course of carbon uptake of Eriophorum vaginatum in a moorland habitat: II. The seasonal course of photosynthesis. J. Ecol. 72 (2), 685–700. https://doi.org/10.2307/2260076.
Rochefort, L., Isselin-Nondedeu, F., Boudreau, S., Poulin, M., 2013. Comparing survey methods for monitoring vegetation change through time in a restored peatland. Wetl. Ecol. Manag. 21 (1), 71–85. https://doi.org/10.1007/s11273-012-9280-4.
Saarnio, S., Winiwarter, W., Leitao, J., 2009. Methane release from wetlands and watercourses in Europe. Atmos. Environ. 43 (7), 1421–1429.
Sarauer, J.L., Coleman, M.D., 2018. Biochar as a growing media component for containerized production of douglas-fir. Can. J. For. Res. 48 (5), 581–588. https://doi.org/10.1139/cjfr-2017-0415.
Shao, S., Wu, J., He, H., Moore, T.R., Bubier, J.L., Larmola, T., Juutinen, S., Roulet, N.T., 2022. Ericoid mycorrhizal fungi mediate the response of ombrotrophic peatlands to fertilization: a modeling study. New Phytol. 238 (1), 80–95. https://doi.org/10.1111/nph.18555.
Silvan, N., Silvan, K., Näkkilä, J., Tahvonen, R., Reinikainen, O., 2012. Renewability, Use and Properties of Sphagnum Biomass for Growing Media Purposes. The 14th International Peat Congress, Peatlands in Balance, pp. 3–8. Book of Abstracts.
Silvan, N., Jokinen, K., Näkkilä, J., Tahvonen, R., 2017. Swift Recovery of Sphagnum Carpet and Carbon Sequestration after Shallow Sphagnum Biomass Harvesting. https://doi.org/10.19189/MAP.2015.OMB.198.
Sonnentag, O., Hufkens, K., Teshera-Sterne, C., Young, A.M., Friedl, M., Braswell, B.H., Milliman, T., O'Keefe, J., Richardson, A.D., 2012. Digital repeat photography for phenological research in forest ecosystems. Agric. For. Meteorol. 152, 159–177. https://doi.org/10.1016/j.agrformet.2011.09.009.
Stan Development Team, 2024. Stan Modeling Language Users Guide and Reference Manual, Version 2.35. https://mc-stan.org/.
Strack, M., Zuback, Y.C.A., 2013. Annual carbon balance of a peatland 10 yr following restoration. Biogeosciences 10 (5), 2885–2896. https://doi.org/10.5194/bg-10-2885-2013.
Strack, M., Keith, A.M., Xu, B., 2014. Growing season carbon dioxide and methane exchange at a restored peatland on the Western Boreal Plain. Ecol. Eng. 64, 231–239. https://doi.org/10.1016/j.ecoleng.2013.12.013.
Strack, M., Mwakanyamale, K., Fard, G.H., Bird, M., Bérubé, V., Rochefort, L., 2016. Effect of plant functional type on methane dynamics in a restored minerotrophic peatland. Plant Soil 410 (1–2), 231–246. https://doi.org/10.1007/s11104-016-2999-6.
Tian, W., Hongmei, W., Xing, X., C, L.P., Xuan, Q., Ruicheng, W., Xianyu, H., H, T.O., 2023. Water table level controls methanogenic and methanotrophic communities and methane emissions in a Sphagnum-dominated peatland. Microbiol. Spectr. 11 (5). https://doi.org/10.1128/spectrum.01992-23.
Tommila, T., Kämäräinen, A., Kokko, H., Palonen, P., 2022. Sphagnum moss is a promising growth substrate in arctic bramble container cultivation. Acta Agric. Scand. Sect. B Soil Plant Sci 72 (1), 997–1008. https://doi.org/10.1080/09064710.2022.2138778.
Triisberg, T., Karofeld, E., Paal, J., 2011. Re-vegetation of block-cut and milled peatlands: an Estonian example. Mires Peat 8 (05), 1–14.
Triisberg, T., Karofeld, E., Paal, J., 2013. Factors affecting the re-vegetation of abandoned extracted peatlands in Estonia: a synthesis from field and greenhouse studies. Est. J. Ecol. 62 (3), 192. https://doi.org/10.3176/eco.2013.3.02.
Tuittila, E.-S., Komulainen, V.-M., Vasander, H., Laine, J., 1999. Restored cut-away peatland as a sink for atmospheric CO 2. Oecologia 120 (4), 563–574. https://doi.org/10.1007/s004420050891.
Tuittila, E., Rita, H., Vasander, H., Laine, J., 2000. Vegetation patterns around *Eriophorum vaginatum* L. Tussocks in a cut-away peatland in southern Finland. Can. J. Bot. 78 (1), 47–58. https://doi.org/10.1139/b99-159.
Upenieks, E.M., Rudusāne, A., 2022. Afforestation as a type of peatland recultivation and assessment of its affecting factors in the reduction of GHG emissions. Rural Development 2021 (1), 295–300. https://doi.org/10.15544/rd.2021.052, 2019.
van der Maaten, L., 2014. Accelerating t-SNE using tree-based algorithms. J. Mach. Learn. Res. 15 (1), 3221–3245. https://doi.org/10.5555/2627435.2697068.
van der Maaten, L., Hinton, G., 2008. Visualizing data using t-SNE. J. Mach. Learn. Res. 9 (11).
van Winden, J.F., Reichart, G.-J., McNamara, N.P., Benthien, A., Damsté, J. S. Sinninghe, 2012. Temperature-induced increase in methane release from peat bogs: a mesocosm experiment. PLoS One 7 (6), e39614. https://doi.org/10.1371/journal.pone.0039614.
Vozbrannaya, A., Antipin, V., Sirin, A., 2022. After wildfires and rewetting: results of 15 + years' monitoring of vegetation and environmental factors in cutover peatland. Diversity 15 (1), 3. https://doi.org/10.3390/d15010003.
Waddington, J.M., Day, S., 2007. Methane emissions from a peatland following restoration. Journal of Geophysical Research Atmospheres 112 (G3). https://doi.org/10.1029/2007jg000400.
Waddington, J.M., McNeil, P., 2002. Peat oxidation in an abandoned cutover peatland. Can. J. Soil Sci. 82 (3), 279–286. https://doi.org/10.4141/S01-043.
Wei, X., Zhang, W., Zulfiqar, F., Zhang, C., Chen, J., 2022. Ericoid mycorrhizal fungi as biostimulants for improving propagation and production of ericaceous plants. Front. Plant Sci. 13. https://doi.org/10.3389/fpls.2022.1027390.
Wickham, H., 2016. Getting started with ggplot2. In: Wickham, H. (Ed.), ggplot2: Elegant Graphics for Data Analysis. Springer International Publishing, pp. 11–31. https://doi.org/10.1007/978-3-319-24277-4_2.
Wilson, D., Alm, J., Laine, J., Byrne, K.A., Farrell, E.P., Tuittila, E., 2009. Rewetting of cutaway peatlands: are we Re-creating hot spots of methane emissions? Restor. Ecol. 17 (6), 796–806. https://doi.org/10.1111/j.1526-100X.2008.00416.x.
Woebbecke, D.M., Meyer, G.E., Von Bargen, K., Mortensen, D.A., 1995. Color indices for weed identification under various soil, residue, and lighting conditions. Transactions of the ASAE 38 (1), 259–269. https://doi.org/10.13031/2013.27838.
Yli-Petäys, M., Laine, J., Vasander, H., Tuittila, E.-S., 2007. Carbon gas exchange of a re-vegetated cut-away peatland five decades after abandonment. Boreal Environ. Res. 12 (3), 177–190.
Yu, Z.C., 2012. Northern peatland carbon stocks and dynamics: a review. Biogeosciences 9 (10), 4071–4085. https://doi.org/10.5194/bg-9-4071-2012.